

Beam Orbit Simulation in the Central Region of the RIKEN AVF Cyclotron

Dragan Toprek, Akira Goto and Yasushige Yano

The Institute of Physical and Chemical Research (RIKEN)

Hirosawa 2-6, Wako-shi, Saitama, 351-01 Japan

Abstract

This paper describes the modification design of the central region for $h = 2$ mode of acceleration in the RIKEN AVF cyclotron. The central region is equipped with an axial injection system. The spiral type inflector is used for axial injection. The electric field distribution in the inflector and in four acceleration gaps has been numerically calculated from an electric potential map produced by the program RELAX3D. The magnetic field is measured. The geometry of the central region has been tested with the computations of orbits carried out by means of the computer code CYCLONE. The optical properties of the spiral inflector and the central region are studied by using the program CASINO and CYCLONE, respectively. We have also made an effort to minimize the inflector fringe field using the RELAX3D program.

1. Introduction

The basic characteristics of the RIKEN AVF cyclotron are described in Refs. [1,2]. Here we repeat them briefly.

The RIKEN AVF cyclotron is a compact isochronous cyclotron with four spiral sectors. The magnetic induction at the centre of the machine varies from 0.5 T to 1.7 T. Its constant is $K = 70 \text{ MeV}$. Extraction radius of the machine is $r_e = 71.4 \text{ cm}$. The ions coming from the ECR ion source (the maximum extraction voltage U_{ex}^{\max} is 13 kV) are injected in the AVF cyclotron axially from up. They are introduced into the median plane of the machine by a tilted spiral inflector. The acceleration then takes place at four electric gaps per turn. The angular span of the dees is 85° . The vertical aperture of the dees inside the central region is 24 mm. The maximum amplitude of the dee voltage is 50 kV and its frequency goes from 12 MHz to 24 MHz. The number of trim coils is 9, and the number of harmonic coils is 1 in the extraction region.

In the Refs. [1,2] is shown the shape of the electrodes of the central region, but in the former design, when the ion trajectory through the spiral inflector (with parameters: $A = 2.6 \text{ cm}$ and $k' = 0.0$) is analytically calculated and the electric field distribution in the four acceleration gaps is described by a gaussian function. Now, to treat more realistically both the spiral inflector and the central region, the electric field distributions in the inflector and in the four accelerating gaps has been numerically calculated from electric potential maps, produced by RELAX3D program [4,5]. For the analysis of the ion trajectories through the spiral inflector and in the central region, which includes both the electric and magnetic fields data, we used the CASINO [6] and CYCLONE [7] programs, respectively. The median plane magnetic field map $B(r, \theta)$, which is the

measured, is stored in a polar mesh with $\Delta\theta = 1.8^\circ$ and $\Delta r = 2 \text{ cm}$.

2. Spiral inflector

Scaling of the trajectories through the spiral inflector demands that the radius of curvature R_m , which the ion would have if it were acted upon by a magnetic field in the absence of any electric field, is constant. The value for R_m is given by the following expression:

$$R_m = \sqrt{\frac{2 \times 10^9 E_0 [\text{MeV}/n] U_{ex} [\text{kV}]}{c^2 \eta B_0^2 [\text{T}]}} = \text{const.}, \quad (1)$$

where: U_{ex} - the extraction voltage of the ion source in kV, B_0 - the center field value in T, η - the specific charge of the ion, $E_0 = mc^2 / A$ - the rest energy of the ion per nucleon in MeV.

The value of R_m for the representative ion ($\eta = 0.357, B_0 = 1.5 \text{ T}, E_0 = 931.5 \text{ MeV}/n, U_{ex} = 10 \text{ kV}$) is $R_m = 1.61 \text{ cm}$. If we want to use the same spiral inflector for another kind of ion, the extraction voltage U_{ex} and the center field value B_0 for that kind of ion can be obtained by scaling according to Eq. (1). We have selected the spiral inflector with following parameters: $A = 2.2 \text{ cm}$ [3] (A is the radius of curvature which the ion would have if it were acted upon by an electric field in the absence of any magnetic field, in fact it is the height of the spiral inflector) and $k' = 0.3$ [3] (k' is a parameter which is related to the direction of the electric field) with the tapered electrodes, trying to minimize the inflector fringe field and the horizontal cross section of the inflector. The electrode spacing at the inflector entrance is $d_0 = 0.8 \text{ cm}$, the width of its electrode is 1.6 cm (aspect ratio is 2) and the maximal electrode potential is $\pm 3.6 \text{ kV}$. The distance between the center of trajectory at the inflector exit and the center of the cyclotron (so called off-center) is $\rho_c = 1.1 \text{ cm}$.

The electric field produced from the electric potential has characteristic fringe field distribution at the ends of the inflector. A real inflector has fringe fields, which increase the effective length of the inflector. We can compensate the entrance fringe field of the inflector by decreasing the voltage between the inflector electrodes or by cutting a certain pieces of the inflector. The fringe fields change the optics of the inflector and push the particles to oscillate around the design line (central trajectory in the case when electric field is analytic [3]) of the inflector. This may be observed by running CASINO [6].

3. Phase space at the entrance and exit of the spiral inflector

The phase space diagram in two transversal planes (u, p_u) and (h, p_h) [3] at the inflector entrance (dashed and dotted line) and at its exit (full line curves marked by letters f_u and f_h respectively) are presented in Fig. 1. Seven particles from the contour in the (u, p_u) and (h, p_h) planes, which correspond to the inflector entrance emittance of $\epsilon_u = 140\pi \text{ mm mrad}$ (dashed line) and $\epsilon_h = 130\pi \text{ mm mrad}$ (dotted line) and the relative change of the longitudinal component of the momentum of the ion at the inflector entrance is $\delta p_v = \Delta p_v / p = -0.01$, $\delta p_v = 0.0$, $\delta p_v = +0.01$, were run through the spiral inflector using the code CASINO [3]. p is the total momentum of the ion in length units.

For each of these three values of δp_v we have three different curves at the inflector exit. Full line curves with full triangle, full circle and full rectangular symbols at the inflector exit correspond to $\delta p_v = -0.01$, $\delta p_v = 0.0$ and $\delta p_v = +0.01$ at the inflector entrance, respectively. Due to the coupling effects we consider the motion of the particles through the spiral inflector in all three planes. Fig. 1a shows the case when the particle is inflected by voltage decreased by 8% ($\Delta s = 0 \text{ mm}$, $\chi = 8\%$) and in Fig. 1b we compared results at the inflector exit when $\Delta s = 0 \text{ mm}$, $\chi = 8\%$ (full line curve with full rectangular symbol) and when the particle is inflected by cutting off 1.5 mm piece of the inflector at its entrance ($\Delta s = 1.5 \text{ mm}$, $\chi = 0\%$ - full line curve with full circle symbol), but $\delta p_v = 0.0$ at inflector entrance.

From Fig. 1b we can see that the differences of the optical properties of our spiral inflector in the case when $\Delta s = 0 \text{ mm}$, $\chi = 8\%$ compared to the case when $\Delta s = 1.5 \text{ mm}$, $\chi = 0\%$ is negligible. Because of that we will consider further only the case when $\Delta s = 0 \text{ mm}$, $\chi = 8\%$.

4. Orbit studies and optical properties of the central region

4.1. Horizontal motion of the central ray

Our results prove that the energy gain corresponding to the central ion trajectory is sufficient to clear all the obstacles successfully, Fig. 2. The trajectories of reference ion ($\eta = 0.357$, $B_0 = 1.5 T$, $h = 2$) for three value of starting phase $\phi_0 = -50^\circ$ (full line), $\phi_0 = -55^\circ$ (dashed line) and $\phi_0 = -60^\circ$ (dotted line) during the first two turns are also presented. The dee voltage is $U_0 = 50 \text{ kV}$. These orbits are the "central rays" (the initial radius of the ion trajectory is $r_0 = 2.26 \text{ cm}$ and the initial radial momentum is

$p_{r0} = 0.67 \text{ cm}$) for different starting phase.

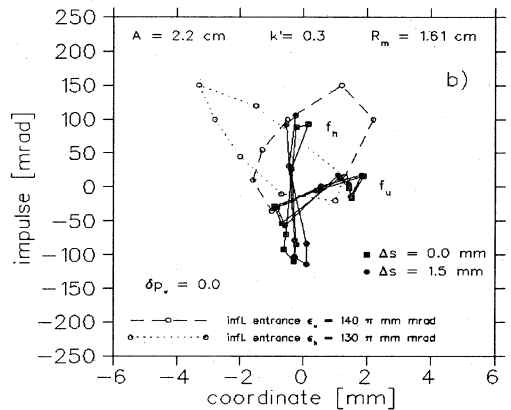
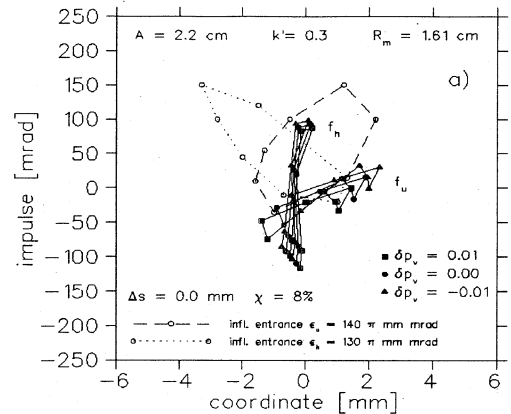


Fig. 1. Phase space diagram in two transversal planes (u, p_u) and (h, p_h) at the inflector entrance (dashed and dotted line) and at its exit (full line curves marked by letters f_u and f_h respectively). The inflector entrance emittance is $\epsilon_u = 140\pi \text{ mm mrad}$ (dashed line) and $\epsilon_h = 130\pi \text{ mm mrad}$ (dotted line) and the relative change of the longitudinal component of the momentum of the ion at inflector entrance is $\delta p_v = -0.01$, $\delta p_v = 0.0$ and $\delta p_v = +0.01$. The others marks are explained in the text.

Fig. 3 shows the modified shape of the electrode in the central region of the RIKEN AVF cyclotron. The dotted area shows the area that has been cutting off of the previously designed electrode, according to the new simulation result.

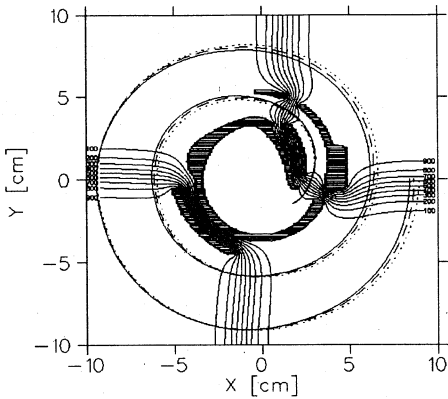


Fig. 2. The central trajectory of the referent ion ($\eta = 0.357$, $B_0 = 1.5 T$, $h = 2$) in the central region of the K70 AVF cyclotron for different value of the starting phase ϕ_0 with the equipotential contours of the numerical calculated field. $\phi_0 = -50^\circ$ (full line), $\phi_0 = -55^\circ$ (dashed line) and $\phi_0 = -60^\circ$ (dotted line). The equipotential contours are plotted at each 10% of the dee voltage U_0 .

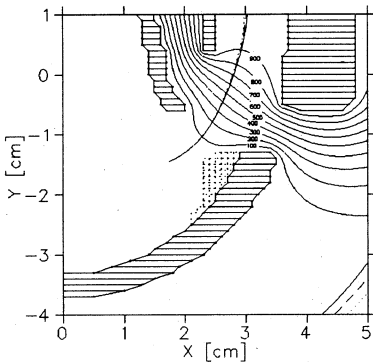


Fig. 3. The modified shape of the electrode in the central region of the RIKEN AVF cyclotron. The dotted area has cut off of the previously designed electrode.

4.2. Vertical motion of the paraxial rays

We tested the phase acceptance of the central region of the machine by following the first two turns of the ions. The emittance of the beam was reconstructed from its emittance at the entrance of the inflector (see Fig. 1a). The family of curves marked by letters f_u and f_h (which correspond to (u, p_u) and (h, p_h) plane at the inflector exit) now correspond to (z, p_z) and (r, p_r) plane, respectively, at the entrance of the central region of the cyclotron.

The maximal axial displacement, defined as the beam envelope, of the trajectories of seven particles defining the contour at the inflector exit, was checked at

each degree in the first two turns. The vertical displacements of the representative ion under consideration for three different starting phase are shown in Fig. 4. Only those starting phase which give vertical envelopes contained within the smallest vertical aperture of the central region are shown. From Fig. 4 we can see that the phase acceptance of the central region is about 10 degrees.

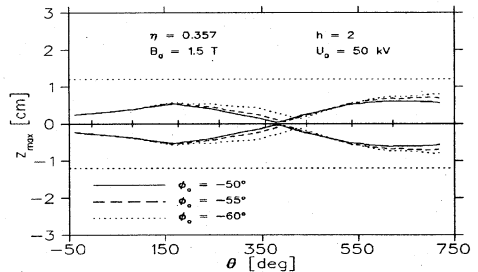


Fig. 4. The maximal vertical displacement of the beam in the first two turns for considered ion in the K70 AVF cyclotron for different value of the starting phase ϕ_0 . The short lines crossing the abscissa show the electric gap positions and the dotted lines parallel to abscissa indicate the minimal vertical aperture of the central region.

6. Conclusions

Our orbit studies through the spiral inflector with following parameters: $A = 2.2 \text{ cm}$, $k' = 0.3$, $R_m = 1.61 \text{ cm}$ shown that the differences of the optical properties of that spiral inflector are negligible in the case when the inflection of the ion is reached by the voltage decreased by 8% and in the case when the inflection of the ion is reached by cutting off a 1.5 mm peace of the inflector at its entrance.

Our orbit studies during the acceleration in the central region of the cyclotron indicated that the clearances between the ion and the solid obstacles and the vertical focusing in the first two turns are satisfactory, but the smaller value for emittance at inflector entrance in both u_r and h_r direction are desirable.

References

- [1] - A. Goto et all, Injector AVF Cyclotron at RIKEN, Proc. 12th Int. Conf. on Cyclotrons and their Applications, Berlin, 1989, p. 51.
- [2] - A. Goto et all, Study of Beam Optics for the Injector AVF Cyclotron at RIKEN, Proc. 12th Int. Conf. on Cyclotrons and their Applications, Berlin, 1989, p. 439.
- [3] - L. W. Root, M.Sc. Thesis, Univ. of British Columbia, 1972.
- [4] - C. J. Kost and F. W. Jones, RELAX3D User's Guide and Reference Manual, TRI-CD-88-01, Vancouver, 1988.
- [5] - Lj. M. Milinkovic, RELAX3D Spiral Injectors, TR30-DN-89-21, Vancouver, 1989.
- [6] - F. B. Milton and J. B. Pearson, CASINO User's Guide and Reference Manual, TRI-DN-89-19, Vancouver, 1989.
- [7] - B. F. Milton, CYCLONE VERS 6.0, TRIUMF Internal Report, June 22, 1989.